Molecular and micro-architectural mapping of abnormal gray matter developmental trajectories in psychosis

Natalia García-San-Martín[1], Richard AI Bethlehem[2], Agoston Mihalik[3], Jakob Seidlitz[4,5], Isaac Sebenius[3], Claudio Alemán-Morrillo[1], Lena Dorfschmidt[4], Golia Shafiei[6], Víctor Ortiz-García de la Foz[7], Kate Merrit[8], Anthony David[8], Sarah E Morgan[3], Miguel Ruiz-Veguilla[9,10], Rosa Ayesa-Arriola[7], Javier Vázquez-Bourgon[7], Aaron Alexander-Bloch[4], Bratislav Misic[11], Edward T Bullmore[3], John Suckling[3], Benedicto Crespo-Facorro[7,9,10], Lifespan Brain Chart Consortium, Rafael Romero-García[1,3,10,*]

1- Department of Medical Physiology and Biophysics, University of Seville, Seville, Spain
2- Department of Psychology, University of Cambridge, Cambridge, UK
3- Department of Psychiatry, University of Cambridge, Cambridge, UK
4- Department of Child and Adolescent Psychiatry and Behavioral Science, The Children's Hospital of Philadelphia, Philadelphia, PA, USA.
5- Lifespan Brain Institute, The Children's Hospital of Philadelphia and Penn Medicine, Philadelphia, PA, USA
6- Department of Psychiatry, Perelman School of Medicine, University of Pennsylvania, Philadelphia, Pennsylvania, USA
7- Department of Psychiatry. Marqués de Valdecilla University Hospital, IDIVAL, School of Medicine, University of Cantabria, Santander, Spain
8- Division of Psychiatry, Institute of Mental Health, UCL, London, UK
9- Mental Health Service, Virgen del Rocío University Hospital, Seville, Spain
10- Instituto de Biomedicina de Sevilla (IBiS) HUVR/CSIC/University of Seville / CIBERSAM, ISCIII, Seville, Spain
11- Montreal Neurological Institute, McGill University, Montreal, Canada

ABSTRACT

The psychosis spectrum encompasses a heterogeneous range of clinical conditions associated with abnormal brain development. The molecular and micro-architectural attributes that account for structural deviations from typical neurodevelopment are still unknown. Here, we aggregate magnetic resonance imaging data from 38,696 healthy controls and 1,256 psychosis-related cases, including first-degree relatives, psychotic experiences, first-episodes, and chronic conditions. Using normative modeling, we generated centile scores for cortical gray matter phenotypes, identifying deviations in regional volumes below the expected trajectory for all conditions. Additionally, we mapped 46 neurobiological features from healthy individuals (including neurotransmitters, cell types, layer thickness, microstructure, cortical expansion, and metabolism) to these centiles using a multivariate approach. Results revealed that neurobiological features were highly co-localized with centile deviations, where metabolism and neurotransmitter concentrations showed the most consistent spatial overlap with abnormal developmental trajectories. These findings shed light on the vulnerability factors that may underlie atypical brain maturation during different stages of psychosis.

INTRODUCTION

Schizophrenia (SCZ) is a severe and chronic psychotic disorder characterized by delusions and hallucinations[1] that has been associated with several risk factors, such as genetic predisposition, substance abuse, and perinatal and early environmental adversities[2]. Family history is an influential vulnerability factor with an estimated heritability of nearly 80%[3]. Accordingly, schizotypal personality disorder, a non-psychotic disorder with schizophrenic traits, is more prevalent among relatives of individuals with SCZ compared to relatives of controls[4]. The presence of subtle cognitive and behavioral abnormalities, as well as a range of cognitive impairments similar to those observed among SCZ patients, has been consistently documented in these non-affected SCZ relatives[5]. In terms of brain structure across different stages of the disorder, individuals with SCZ have shown progressive reductions in cortical gray matter (GM) volume[6,7]. The initial phases of psychosis have also been extensively linked to GM changes in specific regions[8], and the transition to psychosis is further characterized by a progressive loss of volume[9]. Even unaffected first-degree relatives of SCZ patients have shown GM alterations, revealing that genetic factors may play an important role in abnormal brain structure[10].

In addition to SCZ, several clinical diagnostic categories are marked by psychotic symptoms, while the relationship and boundaries among them are still a matter of debate[11]. For instance, schizoaffective disorder (SAD) is a condition characterized by the co-occurrence of schizophrenic symptoms with affective disturbance[1]. It is frequently regarded as a heterogeneous spectrum disorder, with some patients leaning more towards SCZ and others more towards affective disorders. Therefore, there is considerable overlap between SCZ and SAD in terms of symptomatology and treatment[1], showing widespread and overlapping areas of significant GM volume reduction[1]. Nevertheless, the pathophysiological basis of these psychosis-related GM reductions remains unknown[13], and it is still unclear how these findings relate to changes in cortical structure[2].

GM reduction appears to be linked to the pathophysiology of psychosis spectrum onset[3], while such changes may become stable in the chronic stage[4]. Consistent evidence also reveals sex as a differentiating factor in brain structure variability[5]. This interplay of age- and sex-dependent neurodevelopment with specific phases of psychotic disorders has a crucial role in shaping the neurodevelopmental hypothesis of psychosis. An analytical approach capable of handling maturational brain models is necessary to understand this complex dynamic. Identifying deviations in clinical measurements from expected normative values can be achieved using ranked centile scores (e.g., assessment of bone strength[6], metabolic rate[7] , or height and weight measurements commonly used in routine pediatric care). This strategy has been recently extended by Bethlehem et al.[8] which provides reference charts of brain volume to compute individual volumetric centiles normalized by age-, sex- and, importantly, site-effects. Consequently, centile scores provide a standardized and interpretable metric for detecting alterations in regional volumes, thereby contributing to identify patterns of atypical neuroanatomical maturation across psychiatric disorders.

Psychosis has been associated with specific neurobiological alterations, such as neurotransmitters[9,10], metabolism[11], cell type[12,13], and microstructure[14]. Studies on prevalent genetic variations linked to SCZ have consistently pointed towards synaptic function as key factor in terms of disease risk[15]. Specifically, dysregulation of dopaminergic neurotransmission has been detected in SCZ[16], and several neurochemical systems have been suggested to contribute to psychosis pathophysiology, including the glutamate, gamma-aminobutyric acid (GABA), serotonin, and acetylcholine neurotransmitters[9,17]. Complementing the role of neurotransmitters, metabolic and cellular alterations have also been associated with psychosis. Energy metabolism interacts with the disrupted balance of excitatory and inhibitory neurons in

SCZ, which is maintained by glutamatergic and GABAergic signaling[11]; and SCZ patients have demonstrated abnormalities in astroglial[12] and oligodendroglial[13] cells. Regarding microstructure, several abnormalities have been detected in SCZ patients related to myelination, neuropil organization, and expression of proteins that support neurite and synaptic integrity[14,18]. For instance, a magnetic resonance imaging (MRI) marker of intracortical density of myelinated neurons has been associated with genes related to SCZ[19]. Co-localizing these distinctive neurobiological features with structural changes related to stages of psychosis may help understand the common and differential mechanisms involved in the ontology of this disease.

The spatial topography of volume alterations related to psychosis is not uniform across the cortex[20]; instead, certain regions appear to be more susceptible to disease pathology. This observation aligns with the regional vulnerability hypothesis, which posits that local features such as cellular composition[21], neurotransmitter receptors[22], glutamatergic metabolism[23], and gene expression[24] may play a crucial role in the pathophysiology and symptomatology of psychiatric conditions[25]. Within this context of localized susceptibility, recent research has explored the role that brain network dynamics plays in the progression of glioblastoma multiforme[26]; or the influence of network connectivity on vulnerability, resilience, and expression to the onset of SCZ[27]. For example, excessive glutamatergic neurotransmission could lead to excitotoxic cellular damage and death[28], potentially resulting in GM volume reduction[29]. Nevertheless, the understanding of the vulnerabilities that lead to volumetric changes is still limited.

In the present study, we aimed to characterize the molecular and micro-architectural attributes (collectively referred here as neurobiological features) that underlie the pattern of cortical atypical maturation in different psychosis-related groups. We first computed centiles from regional volumes for each group, anticipating that, in line with the neurodevelopmental hypothesis of psychosis, these scores would reveal a pattern of abnormal deviations from normative trajectories. Next, we investigated the regional vulnerability to psychosis through a combined Principal Component Analysis and Canonical Correlation Analysis (PCA-CCA) model for each condition, where centiles were mapped by 46 different neurobiological features: neurotransmitters (19 features), cell types (7), layer thickness (6), microstructure (5), cortical expansion (4), and metabolism (5). Finally, we explored the associations between the inter-regional vulnerability to psychosis across conditions and the neurobiological similarities.

RESULTS

Centiles ranked regional brain volumes of individuals identifying deviations from the expected normative trajectories, while accounting for age, sex, and site-effects (Fig. 1a; see *Methods* for details). Thus, after averaging brain volume across hemispheres for each of the 34 Desikan-Killiany regions[30], centiles were computed for 38,696 healthy controls (HC) and 1,256 individuals classified under eight different psychosis-related diagnoses. First-degree relatives of schizophrenia (*SCZ-relatives*, n = 96) and schizoaffective disorder (*SAD-relatives*, n = 64) were combined to constitute the *SCZ and SAD-relatives* group (Fig. 1b). Individuals who reported operationally-defined psychotic experiences (PEs), whether rated as 'suspected' (*PE-suspected*, n = 48), 'definite' (*PE-definite*, n = 73), or 'clinical' for those who had experienced additional signs of social impairment or help-seeking (*PE-clinical*, n = 36), collectively formed the *PE* group[31,32]. Individuals who experienced a First Episode of Psychosis (FEP, n = 352) composed the *FEP* group. Lastly, individuals diagnosed with chronic schizophrenia (*SCZ*, n = 525) or schizoaffective disorder (*SAD*, n = 62) were combined in the *SCZ and SAD-chronic* group. See *Methods* for subject description, and Supplementary Table 1 for demographic information.

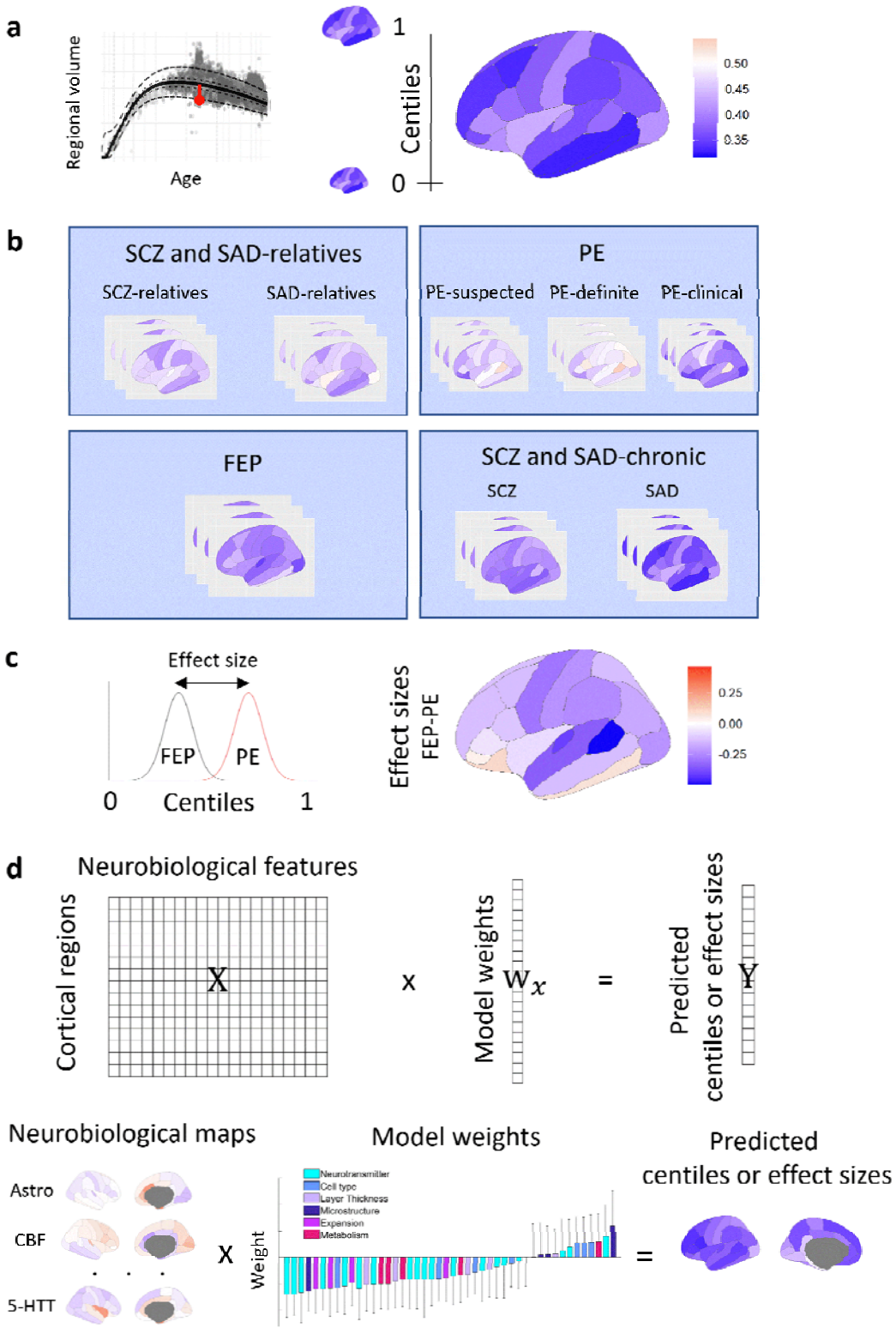

Fig. 1 | Analysis pipeline. Centiles and effect sizes were computed from regional brain volumes, which were then predicted based on combinations of neurobiological features. **a**, Deviation of regional volume from the median volume of neurotypical population for a single

patient (red dot). Resulting ranked deviations, known as centiles, were computed for individuals with the same diagnosis for each brain region defined in the Desikan-Killiany atlas. **b**, MRI data analyzed in the present study included eight different psychosis-related diagnoses organized into four groups according to their clinical profile. **c**, Effect sizes were computed as the Cohen's d between regional centiles for each pair of groups. **d**, Associations between neurobiological maps and empirical centiles (or their effect sizes) were conducted using PCA-CCA modeling which resulted in a set of predicted centiles (or effect sizes) derived from linear combinations of neurobiological features.

Reduction of regional centiles in psychosis-related conditions

We initially computed the mean regional centile distribution (i.e., centile maps) for 8 psychosis-related diagnoses and the 4 groups in which they were clustered (Fig. 2). We found significantly decreased centile scores in global GM volume across all groups (Wilcoxon rank-sum test FDR-corrected; relatives $P = 0.0021$; PE $P = 0.0124$; FEP $P < 10^{-7}$; chronic $P < 10^{-28}$). Compared to HC, SCZ-relatives revealed several significantly reduced regions in association cortices. Although SAD-relatives did not show significant changes in centiles, the group that comprised SCZ and SAD-relatives altogether exhibited a greater number of broadly distributed significant reductions compared to the individual diagnoses. Individuals with 'suspected' and 'definite' PE classifications showed no significant changes in centiles compared to HC, whereas the PE-clinical group exhibited 11 regions significantly reduced. The FEP group, however, exhibited significant differences in all regions compared to HC, except for the inferior temporal and the temporal pole. Lastly, SCZ showed significantly reduced centiles for all regions, while SAD exhibited significant decreases in the majority of them.

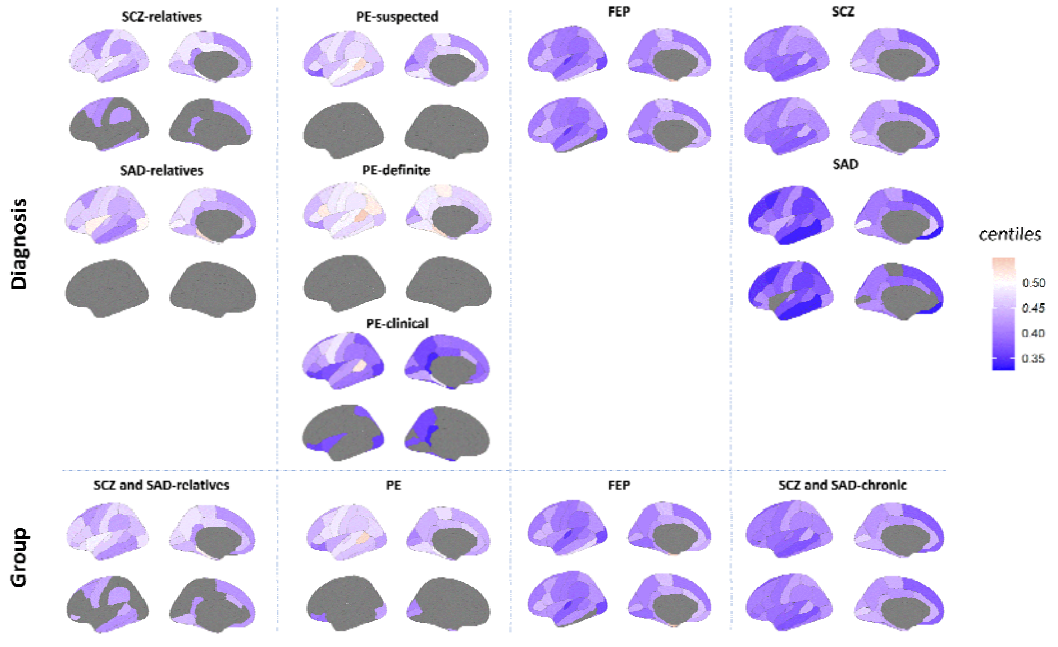

Fig. 2 | Regional brain volume centiles. Regional MRI brain volumes were converted into centiles and subsequently averaged across individuals to generate a mean centile map for each diagnosis and group (first row of each panel). The second row of each panel shows regional

centiles that exhibit significant differences from HC after FDR correction (Wilcoxon rank-sum test, $P < 0.05$).

Differential effect sizes of regional centiles between psychosis-related groups

To determine how centiles vary between psychosis-related groups, we compared the effect size (Cohen's d) between the regional centiles (Fig. 1c) of each pair of psychosis-related groups (Fig. 3). Additionally, we assessed the similarities between centiles of the compared groups by computing the Sum of Squared Differences (SSD) across regions. We tested whether regional effect sizes and SSD significantly differed from zero by performing a permutation test in which group membership was randomly reassigned across the compared groups.

All pairs of groups showed significant differences in centile distributions (Fig. 3 top-right corner; all $P_{perm} < 0.005$), except for SCZ and SAD-relatives versus PE (SSD = 0.054, $P_{perm} = 0.166$). These generalized differences in centiles were also supported by the low regional Pearson correlation between groups (Supplementary Fig. 1; all $P_{perm} > 0.05$). At the regional level, the chronic group exhibited decreased centile values in frontal and temporal lobes compared to the relatives, PE, and FEP. However, in comparison to FEP, the chronic group also showed an increase in the occipital lobe and the transverse temporal region. Lastly, FEP group demonstrated increased centile values in entorhinal, and a decrease in frontal, temporal, and occipital lobe regions compared to the relatives and PE groups.

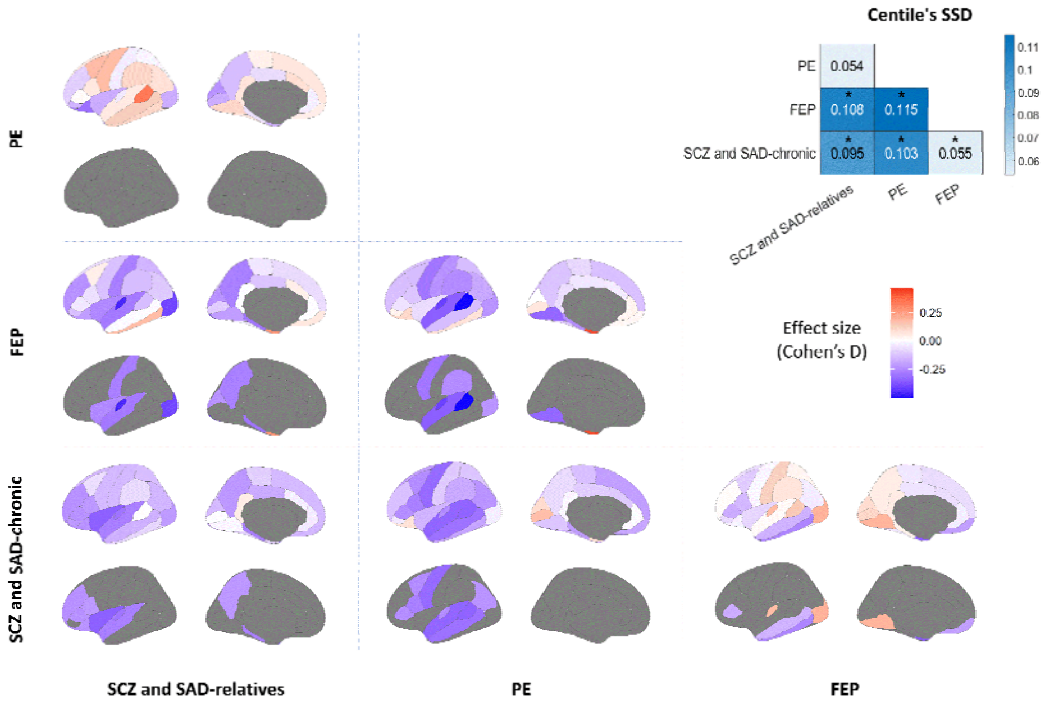

Fig. 3 | Effect sizes of centiles between groups. Cohen's d was computed between regional centiles of each pair of groups to map the effect sizes of centiles between conditions (first row of each panel). The second row of each panel shows regional effect sizes that exhibit significant differences between groups after FDR correction ($P_{perm} < 0.05$). Centile's SSD panel shown at the top-right corner represents the sum of regional centile squared differences

between groups. Asterisks (*) indicate significant differences in SSD between groups (FDR-corrected $P_{perm} < 0.05$).

Mapping neurobiological maps to centiles

A combined Principal Component Analysis (PCA) and Canonical Correlation Analysis (CCA) approach was used as a multivariate method to capture associations between neurobiological maps (X; see Supplementary Table 2 for a complete list of neurobiological features) and regional centiles (Y; Fig. 1d; see *Methods* for details; ref.[33]). The PCA-CCA models determined a set of weights (w_x) through a linear combination (weighted sum) of neurobiological maps, estimating a set of predicted centiles that are, by construction, correlated with the empirical centiles. By employing a spatial permutation test, commonly known as 'spin test', the spherical projections of brain annotation maps were randomly rotated preserving any spatial dependencies[34,35]. This allowed for the identification of significant models and weights while accounting for spatial autocorrelation. Finally, to determine the extent to which each neurobiological feature contributed to the model, a set of loadings was derived by correlating each neurobiological map with the predicted centiles.

Predicted centiles resembled empirical centiles for statistically significant models (Fig. 4a; all groups except PE; FDR-corrected $P_{spin} < 0.05$; see *Supplementary Data* for details). The two clinical groups that showed the lowest regional centiles, FEP, and SCZ and SAD-chronic, also revealed the strongest correlation between predicted and empirical centiles (Fig. 4b; r = 0.63 and r = 0.68, respectively). All significant models exhibited significant loadings (Fig. 4c; $P_{spin} < 0.05$). Specifically, all loadings were negative for the relatives, indicating that the presence of these neurobiological features is highly co-localized with regions that exhibit low centiles. Groups with the lowest centiles, FEP and chronic, showed a greater number of significant loadings, most of which were found to be negative. Synapse density and 5-HT_{2A} demonstrated a large negative contribution for all significant groups. Cortical expansion (Evolutionary exp., Scaling NIH, and Scaling PNC) and neurotransmitters (5-HT_{2A}, $\alpha_4\beta_2$, $mGluR_5$) provided a higher prevalence of negative loadings for the relatives and the chronic group, while metabolism (CBF, $CMRO_2$, CMRGlu) and microstructure (Gene PC1, Myelin (T_1-w/T_2-w), and Synapse density) features predominated negatively in FEP group. Layer thickness loadings (Layers I, II, V, VI) made a significant negative contribution in the chronic group. Conversely, positive loadings indicated a high presence of these neurobiological features in regions closer to neurotypical centiles, or equivalently, a low presence in affected regions. Cell type loadings were both positive (low presence of Micro, OPC, Astro at low centile regions) and negative (high presence of Neuro-Ex, Neuro-In at low centile regions) in FEP. In contrast, 5-HT_6, 5-HTT, D_1, D_2, DAT, H_3, NMDA, VAChT, Endo, Oligo, Layer III, and Neurotransmitter PC1 did not exhibit significant associations with centile changes in psychosis for any of the groups. These loading distributions were similar to those of the weights of the models (Supplementary Fig. 2). Leave-one-study-out cross-validation performed both within the chronic group and SCZ diagnosis indicated that centiles and loadings were not primarily influenced by individual studies (Supplementary Figs. 3-4, respectively). Additionally, empirical and predicted centiles, and associated loadings of each individual diagnosis demonstrated a high consistency across diagnoses classified under the same group (Supplementary Figs. 5-7).

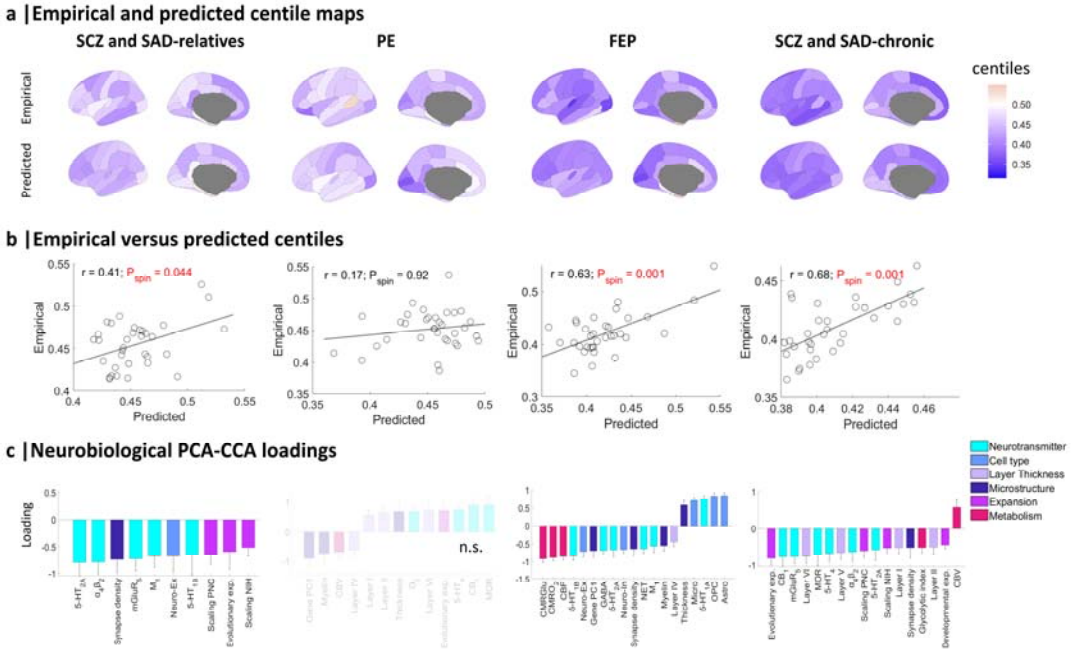

Fig. 4 | Empirical and predicted centiles, and associated loadings from PCA-CCA models. **a**, Maps of empirical MRI-derived centiles (top) and predicted PCA-CCA-derived centiles from neurobiological features (bottom). **b**, Correlation between empirical and predicted regional centiles. **c**, PCA-CCA significant loadings associated to each neurobiological map ($P_{spin} < 0.05$). Non-significant models are denoted as n.s (FDR-corrected $P_{spin} > 0.05$). Error bars represent the standard deviation.

Mapping neurobiological maps to effect sizes of centiles between psychosis-related groups

We additionally assessed the associations between the neurobiological maps (X) and the effect sizes of centiles computed between each pair of groups (Y). Predicted effect sizes closely matched the empirical values for statistically significant models (all group pairs except those involving relatives; FDR-corrected $P_{spin} < 0.05$; see *Supplementary Data* for details), indicating that neurobiological maps partially explain the spatial distribution of centiles across the cortex (Fig. 5; top of each panel).

All significant models provided significant loadings (Fig. 5; bottom of each panel; $P_{spin} < 0.05$). 5-HT_4, CB_1 and MOR (neurotransmitters); Layers I, II and VI; Gene PC1 (microstructure); and CBV (metabolism) were commonly present in chronic versus FEP and PE groups; all of them negatively contributing. On the other hand, FEP group exhibited 5-HT_{1A} and 5-HT_{1B} as significant neurotransmitters; Astro, Micro, Neuro-In and OPC as cell types; and CBF, $CMRO_2$ and CMRGlu as metabolic features in common versus both chronic and PE groups. In PE, 5-HT_{2A} and $\alpha_4\beta_2$ neurotransmitters stood out as common negative loadings versus chronic and FEP individuals. These loading distributions were similar to those of the weights of the models (Supplementary Fig. 8). Furthermore, for significant models, we additionally tested whether neurobiological maps specifically predicted empirical effect sizes using the same permutation test as used for effect sizes and SSD (where group membership was randomly reassigned). Significant differences were observed in FEP versus PE ($P_{perm} = 0.021$; see *Supplementary Data* for details) and chronic versus FEP ($P_{perm} = 0.020$), but not in chronic versus PE ($P_{perm} = 0.13$).

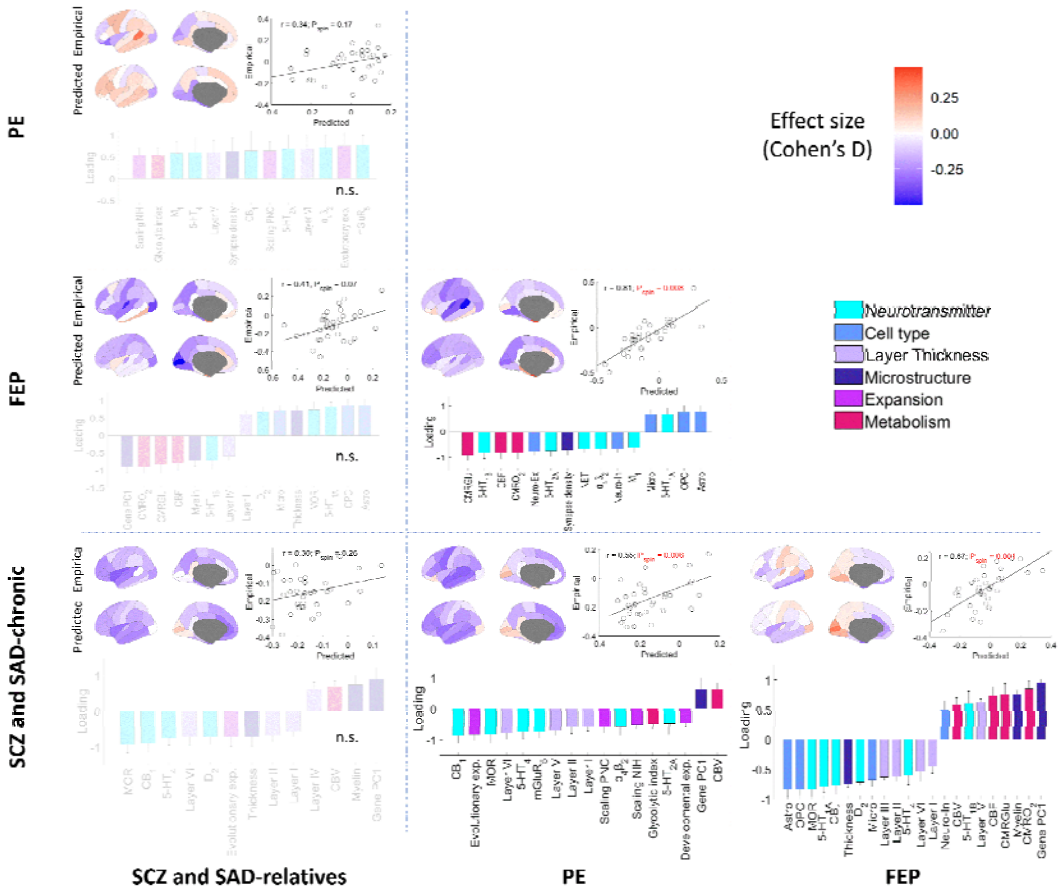

Fig. 5 | Empirical and predicted effect sizes between pairs of psychosis-related groups, and associated loadings from PCA-CCA models. Predicted effect sizes of centiles between groups were derived from neurobiological features using PCA-CCA modeling. Each panel illustrates the empirical and the PCA-CCA predicted effect sizes of centile maps (top-left); the correlation between empirical and predicted effect sizes (top-right); and the neurobiological PCA-CCA significant loadings (bottom; $P_{spin} < 0.05$). Non-significant models are denoted as n.s (FDR-corrected $P_{spin} > 0.05$). Error bars represent the standard deviation.

Comparing neurobiological loadings across psychosis-related groups

We next explored the consistency of loadings described in Fig. 4 by stacking them across groups to reveal potential overlapping features across different conditions (Fig. 6a). The greatest negative loadings indicated a high presence of these features in regions where centiles are consistently low across the four groups. These features included neurotransmitters (from high to low model contribution: 5-HT_{1B}, 5-HT_{2A}, $\alpha_4\beta_2$, NET, GABA, M_1, and 5-HT_6), cell types (Neuro-Ex, Neuro-In), microstructure (Synapse density), and metabolism (CMRGlu, CBF, and $CMRO_2$). On the other hand, the greatest positive loadings, consistent across all groups except chronic, indicated a high presence of these features in regions closer to neurotypical centiles or, equivalently, a low presence in affected regions. These features included neurotransmitters (5-HT_{1A}, 5-HTT, D_2, DAT), cell types (Astro, OPC, Micro), and layer thickness (Layer III). In

contrast to the less severe cases, the chronic group mainly exhibited negative loadings, indicating a generalized presence of features in regions with decreased centiles. These loading distributions were similar to those of the weights of the models (Supplementary Fig. 9).

This shared neurobiological spatial distribution across different psychosis-related groups prompted us to investigate whether regions with similar neurobiological attributes also tend to exhibit overlapping structural vulnerability profiles (centiles). Thus, we created a neurobiological similarity matrix by correlating the neurobiological data across individual regional features (Fig. 6b). We also built a structural co-vulnerability to psychosis matrix by correlating the effect sizes of the centiles across psychosis-related groups. It showed a common inter-regional centile reduction across the psychosis spectrum (median r = 0.52 ± 0.32). The correlation between both matrices revealed a significant association between the neurobiological similarities and the structural co-vulnerabilities to psychosis (Pearson's r = 0.21, $P_{spin} < 10^{-6}$). A significant correlation was also found between the neurobiological similarities and the effect sizes of centiles when considering individual diagnoses instead of groups (Supplementary Fig. 10).

a| Neurobiological loadings stacked by clinical group

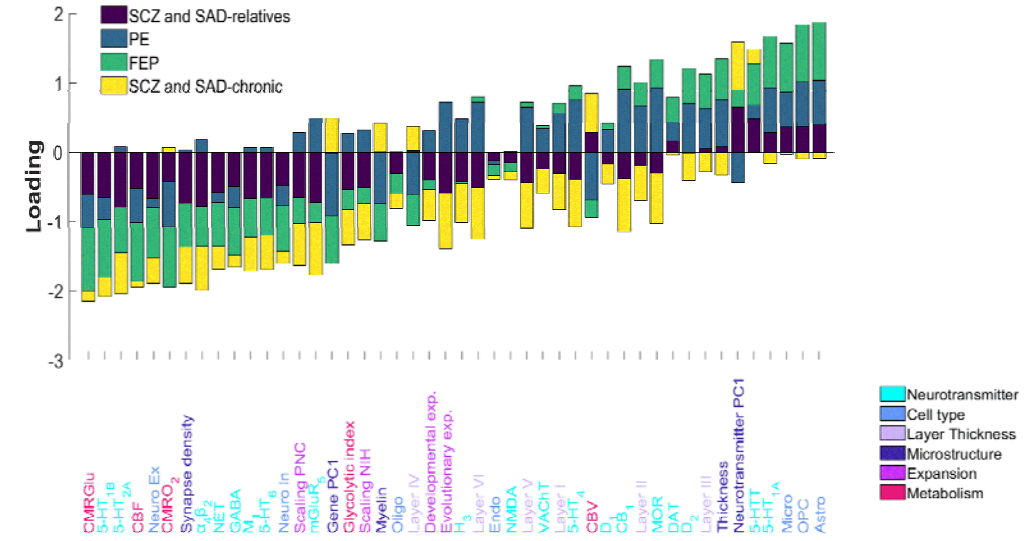

b| Association between neurobiological similarity and structural co-vulnerability to psychosis

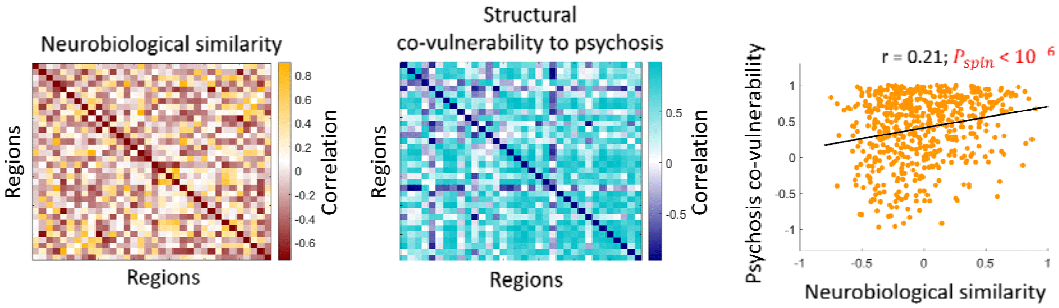

Fig. 6 | Shared neurobiological features among psychosis-related groups. a, Stacked neurobiological loadings of each group, regardless of their significance, were ranked from the most negative to the most positive average contribution. **b,** Neurobiological similarity matrix obtained by correlating the regional patterns of neurobiological features in HC (left). Structural co-vulnerability to psychosis matrix constructed by correlating the regional patterns of the effect sizes of centiles across psychosis-related groups (middle). Association between neurobiological similarity and structural co-vulnerability to psychosis (right).

DISCUSSION

In the present report, we employed a centile-based method to identify, under the neurodevelopmental hypothesis of psychosis, cortical volume deviations below the expected maturational trajectory for different groups of psychosis spectrum (SCZ and SAD-relatives, PE, FEP, and SCZ and SAD-chronic). The predictions of PCA-CCA models captured associations between neurobiological maps and the reduced centiles. This resulted in a set of loadings that reflected how structural changes were co-localized with a set of neurobiological features, providing additional support for the regional vulnerability hypothesis. Accordingly, regions with similar neurobiological attributes also tended to exhibit overlapping profiles of structural vulnerability to psychosis.

Age- and sex-related neurodevelopmental events play a major role in psychotic conditions[36]. Using a centile method that removes age-, sex-, and site-effects[37], we were able to detect brain volume deviations from the expected trajectories. A key benefit of this method, compared to other normative models used in schizophrenia[38,39], lies in its extensive dataset (more than 100,000 scans) that spans the entire lifespan, from 17 post-conception weeks to 100 years. Thus, our centile-based study provides a standardized and interpretable measure of regional brain volume atypicalities for unveiling patterns of neuroanatomical differences across psychiatric disorders that emerge during development and ageing. Here, centiles revealed a significant volume decrease in all psychosis-related groups, with a greater impact on the most severe conditions, FEP and chronic. These results support a continuum view of psychosis psychopathology, as the number of significantly affected regions increased with the severity of the disorder. In particular, FEP, SCZ, and SAD individuals exhibited overlapping GM reductions in frontotemporal and anterior cingulate cortices, which aligns with the reported results in several studies[40–44]. Interestingly, pars orbitalis, a region that is related to mechanisms that lead to volumetric decrease in other cortical regions in SCZ[45], displayed a significant volume reduction in all groups. Decreased centiles shown by relatives compared with HC supports the hypothesis that cortical regions such as cingulate, temporal, and frontal regions may be preferentially affected by the latent genetic liability to SCZ in these asymptomatic individuals[46,47]. On the other hand, the PE group did not show any significant reduction in centiles (only PE-clinical individuals), consistent with previous voxel-based morphometry analyses of the same individuals[48]. This may be attributed to the population diversity (suspected, definite, and clinical PEs), the subclinical nature of the symptoms (only some patients had recurrent PEs; ref. [49]), and the non-specificity of the genetic liability to SCZ, but for a general risk of neuropsychiatric disorders[50]. We also did not find significant centile differences between the two subclinical groups considered: relatives and PE. All other pairs of groups showed significant differences in centile distribution. The decreased centile values in frontal and temporal lobes of the chronic group, compared to the relatives and PE, are consistent with the stage and severity of the disorders as previously reported[40,42]. Compared to FEP, the chronic group showed a decrease in centiles in temporal lobe, and an increase in the occipital lobe. The decrease aligns with the progressive reduction of frontotemporal regions described in

individuals with long-term SCZ[51]. The GM increase in the occipital lobe has also been reported in SCZ patients compared to relatives[52] and to healthy controls[53]. This has been interpreted as a result of brain plasticity attempting to compensate for reduced connectivity[53]. Lastly, the decrease in centiles in the frontal, temporal, and occipital lobes of FEP group compared to relatives and PE groups, supports the relevance of these regions in GM reduction in this early stage of psychosis-related diseases[54,55]. The increased centiles in the entorhinal region supports the hypothesis that the excess activity of the hippocampus, followed by structural degeneration, may be a potential initial locus driving SCZ pathophysiology[56]. Collectively, these findings highlight the presence of reduced centile patterns within each psychosis spectrum disorder, emphasizing the specific and prominent role that abnormal brain maturation plays in the severity of psychosis.

The diagnosis and treatment of these conditions has often presented a challenge due to the heterogeneous nature of these mental disorders, their shared symptomatology, and the limited understanding of the underlying neurobiological mechanisms[16,57,58]. Reductions in GM volume have been associated with several neurobiological features, including variants of the serotonin transporter gene[59], reductions in synaptic density[60] and myelination[61], increases in glucose metabolism[62], as well as astrogliosis and pro-inflammatory cytokines produced by neurons, astrocytes, microglia, and oligodendrocytes[63]. Here, we employed a PCA-CCA multivariate method that assessed differential regional GM vulnerabilities across psychosis-related diagnoses by associating cortical volumes with neurobiological features derived from humans. In this line, recent research has co-localized structural brain development with the underlying neurobiology[64]. Furthermore, the spatial distribution of neurotransmitter receptors and transporters[65], and the connectional hierarchy[66] have been associated with cognitive processes and disease vulnerability. Additionally, a study has suggested that regions that are structurally most vulnerable to disease may also be the most susceptible to rebalance their functional organization through appropriate pharmacological interventions[67].

The large negative contribution of synapse density and 5-HT_{2A} serotonin receptor in all psychosis-related groups indicated a high presence of these features in neurotypical regions that exhibit reduced centiles due to psychosis, supporting the regional vulnerability hypothesis. For example, we found psychosis-related centile reductions in areas with higher synapse density, which is consistent with the loss of synaptic density detected in SCZ patients using a radioligand for synaptic vesicle glycoprotein PET imaging[68]. An abnormal expression pattern of 5-HT_{2A} has been suggested to predispose an individual to the development of psychosis[69] as well as being implicated in the pathogenesis of suicidal behavior through genetic associations in patients with SCZ[70]. In this line, an inverse agonist of 5-HT_{2A} has been discovered to reverse psychosis-like behaviors in a rodent model of Alzheimer's[71] and Parkinson's disease[72]. Additional neurotransmitters that made a negative contribution to the relatives and chronic models included $\alpha_4\beta_2$ nicotinic acetylcholine and $mGluR_5$ glutamate receptors. Studies in rodents have shown that $\alpha_4\beta_2$ agonists enhance sensory gating[73,74], an information processing function that is deficient in SCZ[75]. Pharmacological research in animals has also indicated that $\alpha_4\beta_2$ is involved in multiple cognitive domains impaired in SCZ, including processing speed, visual learning and memory, and social cognition[75]. Pre-clinical evidence has suggested that agonists of the nicotinic $\alpha_4\beta_2$ subtype could be beneficial in improving cognitive function in individuals with SCZ[75,76]. On the other hand, $mGluR_5$ hypoactivity has been observed in SCZ, which may disturb glutamatergic regulation of GABAergic interneurons, supporting the notion of this susceptibility mechanism to the disease[77,78]. We also found consistencies regarding microstructural features beyond synapse density in the FEP group, where negative loadings predominated. According to the literature, changes in cortical myelination and cortical

thickness are co-localized with the expression of genes associated with SCZ[79,80]. The remarkable negative contribution of brain metabolism in FEP may represent a complementary vulnerability mechanism to SCZ. Brain-metabolic features have demonstrated to explain a substantial amount of the variance associated with regional cortical thickness trajectories during childhood and adolescence[64]. Specifically, altered CBF has been found in people at risk for psychosis, in FEP and in SCZ[81]. The negative loading contribution of cortical expansion features in relatives and the chronic group suggests that allometric scaling directly parallels the incidence of neurodevelopmental impairments, as demonstrated in preterm infants[82]. Furthermore, major contributor genes to the rapid evolutionary expansion of the human brain are also significant contributors to SCZ[83]. Layer thickness, a feature related to neuronal density[84,85], also had a significant negative contribution in the chronic group. Moreover, we reported that several cell type loadings contributed positively in FEP. Thus, a high presence of these cell types prevails in regions that closely align with neurotypical centiles, suggesting that their absence might be a contributing factor to vulnerability to the disease. This finding supports the increased complement-mediated microglial pruning and the enhanced phagocytic action of microglial cells produced by astrocytes that has been reported at the onset of SCZ[86].

This study also presents several neurobiological features that concentrates in regions with the largest centile differences between conditions. The differential features of the chronic group versus PE or FEP included a high presence (negative loading) of layer thickness and neurotransmitters such as serotonin, cannabinoid, and opioid receptors. Decreased availability of cannabinoid receptor levels detected in antipsychotic-treated and untreated FEP patients have been associated with greater symptom severity and poorer cognitive functioning in male patients[87]. On the other hand, cerebral blood volume, a metabolism feature that is abnormally elevated and associated with delusions in SCZ[88], stands out for its low presence (positive loading). Features associated with FEP differences with both PE and chronic groups included different neurotransmitters, cell types, and metabolism features, which are, for instance, consistent with the aberrant microglial synaptic pruning that occurs in the early stages of SCZ[89]. Factors that differentiated a PE from FEP or chronic conditions included neurotransmitters, indicating that a greater burden on neurotransmitter signaling may lead to the development of psychosis[90]. These findings potentially contribute to a deeper comprehension of the different molecular mechanisms involved in each psychosis-related group.

Beyond the differential co-localization of neurobiological features found across psychotic conditions, we identified a consistent pattern of overlapping negative loadings across all groups, including neurotransmitters, synapse density, and metabolism. Positive loadings included neurotransmitters, cell types, and Layer III for all groups except chronic, indicating a high presence of these features in regions closer to neurotypical centiles (or, equivalently, a low presence in regions where centiles are low). This overlapping pattern across all groups indicates a high consistency in the features that may be partially responsible for vulnerability to psychosis, supporting the hypothesis of a continuum spectrum for the disorder. The predominance of negative loadings in the chronic group is interpreted as a manifestation of a higher neurobiological vulnerability to abnormal brain development, which is associated with the severity of this stage. These results emphasize the importance of considering each neurobiological feature individually since their co-localization with disease vulnerability is highly specific even within feature subtypes (e.g., 5-HT_{1A} and 5-HT_{1B}). This shared neurobiological vulnerability across different psychosis-related groups led us to investigate the relationship between regions with similar neurobiological attributes and overlapping structural vulnerability profiles (centiles). The significant correlation between the neurobiological

similarities and the structural co-vulnerabilities to psychosis revealed that pairs of regions sharing neurobiological profiles tend to exhibit comparable vulnerabilities across psychotic conditions. In this line, Luppi et al.[67] recently found that inter-regional neurotransmitter similarity was associated with pharmacological susceptibility which, in turn, correlated with a vulnerability pattern to neurological, neurodevelopmental, and psychiatric conditions, reflecting the intrinsic functional architecture of this co-susceptibility.

The present findings must be interpreted with several considerations. First, psychotic disorders were grouped with varying sample sizes and diagnoses, resulting in heterogeneous groups. Nevertheless, it has been suggested that SCZ and SAD patients exhibit overlapping areas of GM reduction[1], and these disorders are even considered neuropsychologically indistinguishable[91]. Additionally, we replicated our findings by considering individual diagnoses instead of groups (Supplementary Figs. 5-7). Second, while abnormalities in relatives, PE, and FEP individuals are not influenced by medication, antipsychotic drugs in chronic individuals may impact cortical volume. Third, neurobiological data used here were derived from normative non-psychotic individuals. Future work with a neurobiological atlas of individuals with schizophrenia could provide new insights into the molecular alterations causally associated with abnormal brain development. Fourth, even though PCA-CCA models determine a set of weights that maximize the correlation between an independent latent variable (i.e., neurobiological maps multiplied by model weights) and a dependent latent variable (i.e., empirical centiles after dimensionality reduction), we focused on loadings instead of reporting these weights since their ease of interpretation, as they depict the relationship between each neurobiological map and the latent variable. Additionally, loadings and centiles were generally similar (see resemblance between Fig. 4c and Supplementary Fig. 2; Fig. 5 and Supplementary Fig. 8; and Fig. 6a and Supplementary Fig. 9).

In summary, we identified group-specific volume deviations below the expected trajectory for different psychosis-related conditions based on centiles. We revealed an overlapping spatial distribution of the neurobiological features, which were highly co-localized with the abnormal developmental trajectories. Altogether, these findings contribute to our understanding of the vulnerability factors that may underlie atypical brain maturation in different conditions and stages of psychosis, which could help define subtypes for future imaging-first molecular phenotyping.

METHODS

Subjects

Magnetic Resonance Imaging (MRI) data were analyzed from eight psychosis-related diagnoses, which were then clustered into four groups according to their clinical profile. MRI from first-degree relatives of schizophrenia (SCZ-relatives; n = 96; age = 43.75 ± 15.25) and schizoaffective disorder (SAD-relatives; n = 64; age = 40.00 ± 16.20), clustered under SCZ and SAD-relatives group; along with chronic schizophrenia (SCZ; n = 525 ; age = 37.63 ± 12.06) and schizoaffective disorder (SAD; n = 62 ; age = 33.77 ± 10.78) subjects, clustered under SCZ and SAD-chronic group, were obtained from Adolescent Brain Cognitive Development (ABCD; refs. [92,93]), Australian Schizophrenia Research Bank (ASRB; ref. [94]), Bipolar-Schizophrenia Network on Intermediate Phenotypes (B-SNIP; ref. [95]), UCLA Consortium for Neuropsychiatric Phenomics (CNP) LA5c Study[96], Mental Illness and Neuroscience Discovery (MIND) Institute Clinical Imaging Consortium (MCIC; ref. [97]), and UK Biobank (UKB; ref. [98]). To be included in the chronic group, patients had to meet DSM-IV diagnostic criteria for schizophrenia or

schizoaffective disorder, which require the presence of at least two psychotic symptoms that are present for a significant portion of time during a 1-month period. Healthy controls (HC; n = 38,232; age = 51.91 ± 23.68) comprised individuals from previous datasets without any current or previous psychotic disorder.

Individuals who were suspected of having had psychotic experiences (PEs; *PE-suspected*; n = 48; age = 21.55 ± 1.06), or were rated as definitely having PEs (*PE-definite*; n = 73; age = 21.75 ± 1.59), or have suffered PEs with social decline and/or help-seeking (*PE-clinical*; n = 36; age = 20.89 ± 0.92) were clustered under the PE subclinical group. All these individuals were sourced from Avon Longitudinal Study of Parents and Children (ALSPAC; refs. [99,100]) birth cohort. Subjects were assessed for PE using the psychotic-like symptoms (PLIKS; refs. [101,102]) semi-structured interview, conducted by trained psychologists[48]. Those who had one or more PE at age 18 years were invited to undergo scanning. The presence of PEs was judged according to clinical criteria of the Schedule for Clinical Assessment in Neuropsychiatry (SCAN; ref. [103]). Randomly selected controls (HC; n = 269; age = 22.30 ± 1.46), from the same cohort who had undergone the same assessments but who were rated as not having had PE experiences, were also scanned.

MRI data from individuals who were determined to have experienced a First Episode of Psychosis (FEP; n = 352; age = 31.43 ± 8.78), along with their respective healthy controls (HC; n = 195; age = 30.64 ± 7.66), were obtained from *Programa de Atención a las Fases Iniciales de Psicosis* (PAFIP; ref. [104]). Patients were initially screened for the presence of psychotic symptoms. Scanning was performed prior to the initiation of any antipsychotic medication[104,105]. All diagnoses were made by an experienced psychiatrist using the Structured Clinical Interview for DSM-IV (SCID-I; ref. [106]) after 6 months of the baseline visit, confirming the presence of schizophrenia or other primary psychotic disorder (refs. [107,108]).

Additional inclusion and exclusion criteria can be found in *Supplementary Information*. See Supplementary Table 1 for demographic details.

MRI acquisition, parcellation and volume extraction

High-resolution brain MRI scans were obtained on different MRI scanners (1.5 – 3T) and acquisition protocols (see *Supplementary Information* for details). T_1-weighted images were acquired with sequences tailored to the respective scanner specifications, and the imaging parameters differed among studies. If both T_1- and T_2/FLAIR-weighted raw data were available, they were processed using FreeSurfer (http://surfer.nmr.mgh.harvard.edu) applying the combined T_1-T_2 recon-all pipeline to enhance gray-white matter boundary delineation. In cases where only raw T_1-weighted data were available, data were processed using the standard recon-all pipeline with FreeSurfer. Briefly, the first processing stage of recon-all includes: non-uniformity correction, projection to Talairach space, intensity normalization, skull-stripping, automatic tissue and subcortical segmentation. Subsequently, surface interpolation, tessellation and registration are done at the second and third stages of the recon-all pipeline.

Cortical brain parcellation was performed using Desikan-Killiany atlas[30], and volumetric measurements were derived for each of the 34 region-of-interest (ROI) defined in the atlas. Volumes were quantified in standardized units (e.g., mm^3) within the respective dataset. Quality control procedures were implemented within each study to ensure the accuracy and reliability of the derived cerebral volumes. Any data exhibiting significant artifacts or processing errors were identified and excluded from further analysis within the specific dataset.

Centile and effect sizes estimation and analysis

To benchmark regional volumes of each psychosis-related diagnosis and group against normative trajectories, we used a generalized additive model for location, scale, and shape (GAMLSS, ref. [37]). This model, available at https://github.com/brainchart/Lifespan, estimated cross-sectional normative age-related trends from 100 different studies (around 100,000 participants; ref. [8]). Therefore, age-normed and sex-stratified measures of brain structure atypicalities across the lifespan, known as centiles, could be derived. Centiles ranked regional brain volumes within a range of 0 (lowest volume) to 1 (highest volume). For example, a subject at the 20th centile would have a volume that is "approximately" lower than 80% of individuals of the same age and sex after adjusting for scanning site offset. Although this constitutes an intuitive interpretation, it is important to note that centiles are based on the GAMLSS models fitted to the data, not on the actual ranking of subjects. Here, therefore, we computed the regional centiles for each individual in our cohorts.

Regional centiles of each diagnosis were compared with healthy controls (HC) using the Wilcoxon rank-sum test, given their inherent non-normal distribution. Additionally, Benjamini-Hochberg false discovery rate (FDR) correction across brain regions was applied to account for multiple comparisons[109]. Centile distributions were averaged for individuals according to their clinical profile to constitute each of the four psychosis-related groups considered here. Global and regional centiles of each group were also compared with HC using the Wilcoxon rank-sum test. Differences between groups were assessed by calculating for each pair of groups: (1) the Cohen's d effect size of centiles; and (2) the Sum of Squared Differences (SSD) between the centiles. To statistically assess these differences in centiles across psychosis-related groups, a permutation test was applied for each pair of group comparisons by randomly shuffling group assignment to create a null distribution of regional centile effect sizes and SSD (10,000 permutations).

Neurobiological cortical maps

We expanded the methodology proposed by Hansen et al.[65] to explore potential associations between cortical volume centile profiles and the spatial maps of 46 molecular and micro-architectural attributes (collectively referred here as neurobiological features) collected across multiple studies. To obtain these maps in their native spaces we used *neuromaps* toolbox available at https://github.com/netneurolab/neuromaps[110].

Neurobiological maps were classified under 6 different types of neurobiological features (see Supplementary Table 2 for a complete list of neurobiological features; ref. [111]): neurotransmitter (19 features), cell type (7), layer thickness (6), microstructure (5), cortical expansion (4), and metabolism (5). Neurotransmitter maps included 19 different neurotransmitter receptors and transporters across 9 different neurotransmitter systems, including serotonin (5-HT$_{1A}$, 5-HT1$_B$, 5-HT$_{2A}$, 5-HT$_4$, 5-HT$_6$, 5-HTT), histamine (H$_3$), dopamine (D$_1$, D$_2$, DAT), norepinephrine (NET), acetylcholine ($\alpha_4\beta_2$, M$_1$, VAChT), cannabinoid (CB$_1$), opioid (MOR), glutamate (mGluR$_5$, NMDA), and GABA. Cell type maps included astrocytes (Astro), endothelial cells (Endo), microglia (Micro), oligodendrocytes (Oligo), oligodendrocytes precursors (OPC), excitatory neurons (Neuro-Ex), and inhibitory neurons (Neuro-In). Cortex thickness was also subdivided into distinct layers (Layers I, II, III, IV, V and VI). Regarding microstructure, the features that belonged to this type were T$_1$-w/T$_2$-w (a proxy measure for intra-cortical myelin; referred to as Myelin in this study), cortical thickness (Thickness), gene expression PC1 (Gene PC1), neurotransmitter PC1, and synapse density. The cortical expansion type was composed by evolutionary expansion (Evolutionary exp.), developmental expansion (Developmental exp.), and allometric scaling from Philadelphia Neurodevelopmental Cohort

(Scaling PNC) and from National Institutes of Health (Scaling NIH). Lastly, cerebral blood flow (CBF), cerebral blood volume (CBV), cerebral metabolic rate of oxygen ($CMRO_2$), cerebral metabolic rate of glucose (CMRGlu) and glycolytic index were classified as metabolism features.

Principal Component Analysis - Canonical Correlation Analysis (PCA-CCA)

A combined Principal Component Analysis (PCA) and Canonical Correlation Analysis (CCA) approach was employed to relate neurobiological maps to regional centiles. CCA is a powerful multivariate method for capturing associations between 2 modalities of data (e.g., brain and behavior; ref. [33]). However, when the sample size (34 cortical regions) is similar to or smaller than the number of variables (46 neurobiological features), standard multivariate models may overfit. To address this problem, a prior dimensionality reduction with PCA was performed. For this purpose, PCA-CCA was executed for different explained variances (60, 70, 80 and 90%). To assess the statistical significance of the models, a spatial autocorrelation-preserving permutation test, termed 'spin test', was used for each of the four variances considered. The spin test projects brain regions to a sphere using spherical coordinates generated during cortical-surface extraction. These spherical projections of brain annotation maps are rotated to randomize the relationship between cortical attributes and annotations[34,35]. Each coordinate is assigned to its nearest rotated counterpart, resulting in an annotated map where spatial autocorrelation is preserved, while the correspondence between parcels and annotations is randomized. Parcels that were closest to the medial wall were assigned the value of the nearest neighboring parcel instead. This procedure was performed at parcel resolution, rather than the vertex resolution, to prevent data upsampling, and it was repeated 10,000 times to generate a parcellation-specific rotation matrix (available at https://github.com/frantisekvasa/rotate_parcellation). To minimize the risk of overfitting, the model selected for each PCA-CCA analysis was the one with the lowest explained variance that was significant according to the spin test (FDR-corrected; see *Supplementary Data*). For non-significant models, the model with lowest explained variance (60%) was selected for illustrative proposes only.

For each of the psychotic group analyses, the PCA-CCA model identified a set of weights (w_x) that maximized the correlation between an independent latent variable (i.e., neurobiological maps multiplied by model weights) and a dependent latent variable (i.e., empirical centiles after dimensional reduction). Thus, the resulting linear combination (weighted sum) of the neurobiological maps constituted a set of predicted centiles that are, by construction, correlated with the empirical centiles. To assess the significance of the model weights, the autocorrelation-preserving spin test, described earlier, was employed. To estimate the standard errors, we created 1,000 bootstrap samples by sampling with replacement the observations of the molecular maps. A potential complication when using bootstrap methods is that resampling may result in alterations in (1) the order of the latent variables that are extracted with each permutation (axis rotation), or (2) the sign of the saliences for each bootstrap sample (reflection; ref. [112]). A Procrustes rotation was used to correct for these rotations and reflections[113]. Finally, to ascertain the extent to which each neurobiological feature contributed to the predicted centiles, a set of loadings was computed. Specifically, the loading associated with each neurobiological feature was defined as the Pearson correlation between the neurobiological map and the predicted centiles.

Neurobiological similarity and structural co-vulnerability to psychosis matrices

Neurobiological features were correlated across regions to obtain a region-by-region matrix of "neurobiological similarity". Simultaneously, a 34-by-4 matrix was constructed to represent structural disorder abnormality based on the regional effect sizes of the centiles for each group. This matrix was further correlated to evaluate the extent to which each pair of regions exhibited similar effects across different groups, resulting in a 34-by-34 matrix referred to as "structural co-vulnerability to psychosis". Subsequently, both the "neurobiological similarity" and "structural co-vulnerability to psychosis" matrices were correlated to identify associations between regions with similar neurobiological attributes and overlapping structural vulnerability profiles (centiles). The same procedure was followed to represent structural disorder abnormality based on the regional effect sizes of the centiles for each diagnosis (rather than group). This was then correlated to obtain the "structural co-vulnerability to psychosis" matrix, and lastly, this matrix was correlated with the "neurobiological similarity" matrix.

DATA AVAILABILITY

Volumetric MRI images from the ALSPAC dataset are available at https://www.bristol.ac.uk/alspac/researchers/access/. PAFIP data are available from the corresponding author on request. The ABCD dataset is available at https://nda.nih.gov/abcd/. ASRB data is supported by Neuroscience Research Australia (NeuRA), available at https://neura.edu.au/resources-tools/asrb. The B-SNIP dataset is available at https://nda.nih.gov/edit_collection.html?id=2274. The LA5c dataset was obtained from the OpenfMRI database (https://legacy.openfmri.org/dataset/ds000030/). MCIC data is available at https://coins.trendscenter.org/, and UKB dataset at https://www.ukbiobank.ac.uk/. The Desikan–Killiany parcellation atlas was obtained from netneurotools (https://github.com/netneurolab/netneurotools).

CODE AVAILABILITY

All code used to perform the analyses can be found at https://github.com/RafaelRomeroGarcia/NeurobiologyCentilesPsychosis. The code used for the PCA-CCA analyses is available at https://github.com/anaston/cca_pls_toolkit.

REFERENCES

1. Amann, B. L. *et al.* Brain structural changes in schizoaffective disorder compared to schizophrenia and bipolar disorder. *Acta Psychiatrica Scandinavica* **133**, 23–33 (2016).

2. Alfimova, M. & Uvarova, L. Cognitive peculiarities in relatives of schizophrenic and schizoaffective patients: heritability and resting EEG-correlates. *International Journal of Psychophysiology* **49**, 201–216 (2003).

3. Cannon, T. D. *et al.* Progressive reduction in cortical thickness as psychosis develops: A multisite longitudinal neuroimaging study of youth at elevated clinical risk. *Biological Psychiatry* **77**, 147–157 (2015).

4. Takahashi, T. & Suzuki, M. Brain morphologic changes in early stages of psychosis: Implications for clinical application and early intervention. *Psychiatry and Clinical Neurosciences* **72**, 556–571 (2018).

5. Kaczkurkin, A. N., Raznahan, A. & Satterthwaite, T. D. Sex differences in the developing brain: insights from multimodal neuroimaging. *Neuropsychopharmacology* vol. 44 71–85 Preprint at https://doi.org/10.1038/s41386-018-0111-z (2019).

6. Yu, F. *et al.* Age-, Site-, and Sex-Specific Normative Centile Curves for HR-pQCT-Derived Microarchitectural and Bone Strength Parameters in a Chinese Mainland Population. *Journal of Bone and Mineral Research* **35**, 2159–2170 (2020).

7. Watson, L. *et al.* Centile reference chart for resting metabolic rate through the life course. *Archives of Disease in Childhood* (2023) doi:10.1136/archdischild-2022-325249.

8. Bethlehem, R. A. I. *et al.* Brain charts for the human lifespan. *Nature* **604**, 525–533 (2022).

9. Yadav, M., Kumar, N., Kumar, A., Jindal, D. K. & Dahiya, M. Possible Biomarkers and Contributing Factors of Psychosis: a Review. *Current Pharmacology Reports* **7**, 123–134 (2021).

10. Merritt, K. *et al.* Variability and magnitude of brain glutamate levels in schizophrenia: a meta and mega-analysis. *Molecular Psychiatry* (2023) doi:10.1038/s41380-023-01991-7.

11. Stein, A., Zhu, C., Du, F. & Öngür, D. Magnetic Resonance Spectroscopy Studies of Brain Energy Metabolism in Schizophrenia: Progression from Prodrome to Chronic Psychosis. *Current Psychiatry Reports* Preprint at https://doi.org/10.1007/s11920-023-01457-1 (2023).

12. Goetzl, E. J. *et al.* Decreased mitochondrial electron transport proteins and increased complement mediators in plasma neural-derived exosomes of early psychosis. *Translational Psychiatry* **10**, (2020).

13. Chew, L. J., Fusar-Poli, P. & Schmitz, T. Oligodendroglial alterations and the role of microglia in white matter injury: Relevance to schizophrenia. in *Developmental Neuroscience* vol. 35 102–129 (S. Karger AG, 2013).

14. Nazeri, A., Schifani, C., Anderson, J. A. E., Ameis, S. H. & Voineskos, A. N. In Vivo Imaging of Gray Matter Microstructure in Major Psychiatric Disorders: Opportunities for Clinical Translation. *Biological Psychiatry: Cognitive Neuroscience and Neuroimaging* vol. 5 855–864 Preprint at https://doi.org/10.1016/j.bpsc.2020.03.003 (2020).

15. Aryal, S. *et al.* Deep proteomics identifies shared molecular pathway alterations in synapses of patients with schizophrenia and bipolar disorder and mouse model. *Cell Reports* **42**, (2023).

16. Howes, O. D. *et al. Mechanisms Underlying Psychosis and Antipsychotic Treatment Response in Schizophrenia: Insights from PET and SPECT Imaging. Current Pharmaceutical Design* vol. 15 (2009).

17. Yang, A. C. & Tsai, S. J. New targets for schizophrenia treatment beyond the dopamine hypothesis. *International Journal of Molecular Sciences* vol. 18 Preprint at https://doi.org/10.3390/ijms18081689 (2017).

18. Stauffer, E. M. *et al.* Grey and white matter microstructure is associated with polygenic risk for schizophrenia. *Molecular Psychiatry* **26**, 7709–7718 (2021).

19. Romero-Garcia, R. *et al.* Schizotypy-Related Magnetization of Cortex in Healthy Adolescence Is Colocated With Expression of Schizophrenia-Related Genes. *Biological Psychiatry* **88**, 248–259 (2020).

20. Cannon, T. D. *et al.* Cortex mapping reveals regionally specific patterns of genetic and disease-specific gray-matter deficits in twins discordant for schizophrenia. *Proceedings of the National Academy of Sciences* **99**, 3228–3233 (2002).

21. Hannon, E. *et al.* Dna methylation meta-analysis reveals cellular alterations in psychosis and markers of treatment-resistant schizophrenia. *eLife* **10**, 1–53 (2021).

22. Chatterjee, M., Verma, R., Ganguly, S. & Palit, G. Neurochemical and molecular characterization of ketamine-induced experimental psychosis model in mice. *Neuropharmacology* **63**, 1161–1171 (2012).

23. Wang, A. M. *et al.* Assessing Brain Metabolism with 7-T Proton Magnetic Resonance Spectroscopy in Patients with First-Episode Psychosis. *JAMA Psychiatry* **76**, 314–323 (2019).

24. Arnatkevičiūtė, A., Fulcher, B. D. & Fornito, A. A practical guide to linking brain-wide gene expression and neuroimaging data. *NeuroImage* **189**, 353–367 (2019).

25. Fusar-Poli, P. *et al.* Neuroanatomy of vulnerability to psychosis: A voxel-based meta-analysis. *Neuroscience and Biobehavioral Reviews* vol. 35 1175–1185 Preprint at https://doi.org/10.1016/j.neubiorev.2010.12.005 (2011).

26. Romero-Garcia, R. *et al.* Transcriptomic and connectomic correlates of differential spatial patterning among gliomas. *Brain* **146**, 1200–1211 (2023).

27. Wei, Q. *et al.* The role of altered brain structural connectivity in resilience, vulnerability, and disease expression to schizophrenia. *Progress in Neuro-Psychopharmacology and Biological Psychiatry* **101**, (2020).

28. Krystal, J. H. *et al.* Impaired Tuning of Neural Ensembles and the Pathophysiology of Schizophrenia: A Translational and Computational Neuroscience Perspective. *Biological Psychiatry* vol. 81 874–885 Preprint at https://doi.org/10.1016/j.biopsych.2017.01.004 (2017).

29. Cahn, W. *et al.* Psychosis and brain volume changes during the first five years of schizophrenia. *European Neuropsychopharmacology* **19**, 147–151 (2009).

30. Desikan, R. S. *et al.* An automated labeling system for subdividing the human cerebral cortex on MRI scans into gyral based regions of interest. *NeuroImage* **31**, 968–980 (2006).

31. Drakesmith, M. *et al.* Mediation of developmental risk factors for psychosis by white matter microstructure in young adults with psychotic experiences. *JAMA Psychiatry* **73**, 396–406 (2016).

32. Merritt, K. *et al.* The impact of cumulative obstetric complications and childhood trauma on brain volume in young people with psychotic experiences. *Molecular Psychiatry* (2023) doi:10.1038/s41380-023-02295-6.

33. Mihalik, A. *et al.* Canonical Correlation Analysis and Partial Least Squares for Identifying Brain–Behavior Associations: A Tutorial and a Comparative Study. *Biological Psychiatry: Cognitive Neuroscience and Neuroimaging* vol. 7 1055–1067 Preprint at https://doi.org/10.1016/j.bpsc.2022.07.012 (2022).

34. Markello, R. D. & Misic, B. Comparing spatial null models for brain maps. *NeuroImage* **236**, (2021).

35. Váša, F. & Mišić, B. Null models in network neuroscience. *Nature Reviews Neuroscience* **23**, 493–504 (2022).

36. Huang, A. S. *et al.* Characterizing effects of age, sex and psychosis symptoms on thalamocortical functional connectivity in youth. *NeuroImage* **243**, (2021).

37. Stasinopoulos, D. M. & Rigby, R. A. Generalized Additive Models for Location Scale and Shape (GAMLSS) in R. *Journal of Statistical Software* **23**, (2007).

38. Wolfers, T. *et al.* Mapping the Heterogeneous Phenotype of Schizophrenia and Bipolar Disorder Using Normative Models. *JAMA Psychiatry* **75**, 1146–1155 (2018).

39. Gur, R. C. *et al.* Neurocognitive growth charting in psychosis spectrum youths. *JAMA Psychiatry* **71**, 366–374 (2014).

40. Maggioni, E., Bellani, M., Altamura, A. C. & Brambilla, P. Neuroanatomical voxel-based profile of schizophrenia and bipolar disorder. *Epidemiology and Psychiatric Sciences* **25**, 312–316 (2016).

41. Calvo, A., Delvecchio, G., Altamura, A. C., Soares, J. C. & Brambilla, P. Gray matter differences between affective and non-affective first episode psychosis: A review of Magnetic Resonance Imaging studies. *Journal of Affective Disorders* **243**, 564–574 (2019).

42. Ivleva, E. I. *et al.* Brain gray matter phenotypes across the psychosis dimension. *Psychiatry Research - Neuroimaging* **204**, 13–24 (2012).

43. van Erp, T. G. M. *et al.* Cortical Brain Abnormalities in 4474 Individuals With Schizophrenia and 5098 Control Subjects via the Enhancing Neuro Imaging Genetics Through Meta Analysis (ENIGMA) Consortium. *Biological Psychiatry* **84**, 644–654 (2018).

44. Liloia, D. *et al.* Updating and characterizing neuroanatomical markers in high-risk subjects, recently diagnosed and chronic patients with schizophrenia: A revised coordinate-based meta-analysis. *Neuroscience and Biobehavioral Reviews* vol. 123 83–103 Preprint at https://doi.org/10.1016/j.neubiorev.2021.01.010 (2021).

45. Zugman, A. *et al.* Structural covariance in schizophrenia and first-episode psychosis: An approach based on graph analysis. *Journal of Psychiatric Research* **71**, 89–96 (2015).

46. Ohi, K. *et al.* Cognitive clustering in schizophrenia patients, their first-degree relatives and healthy subjects is associated with anterior cingulate cortex volume. *NeuroImage: Clinical* **16**, 248–256 (2017).

47. Goghari, V. M., Rehm, K., Carter, C. S. & MacDonald, A. W. Regionally specific cortical thinning and gray matter abnormalities in the healthy relatives of schizophrenia patients. *Cerebral Cortex* **17**, 415–424 (2007).

48. Drakesmith, M. *et al.* Volumetric, relaxometric and diffusometric correlates of psychotic experiences in a non-clinical sample of young adults. *NeuroImage: Clinical* **12**, 550–558 (2016).

49. Sullivan, S. A. *et al.* A population-based cohort study examining the incidence and impact of psychotic experiences from childhood to adulthood, and prediction of psychotic disorder. *American Journal of Psychiatry* **177**, 308–317 (2020).

50. Legge, S. E. *et al.* Association of Genetic Liability to Psychotic Experiences with Neuropsychotic Disorders and Traits. *JAMA Psychiatry* **76**, 1256–1265 (2019).

51. Zhao, Y. *et al.* Cortical Thickness Abnormalities at Different Stages of the Illness Course in Schizophrenia: A Systematic Review and Meta-analysis. *JAMA Psychiatry* vol. 79 560–570 Preprint at https://doi.org/10.1001/jamapsychiatry.2022.0799 (2022).

52. Cao, X. Brain structural alterations in schizophrenia and their non-affected relatives: A voxel-based morphometric study. in *Proceedings - 2020 2nd International Conference on Information Technology and Computer Application, ITCA 2020* 604–608 (Institute of Electrical and Electronics Engineers Inc., 2020). doi:10.1109/ITCA52113.2020.00132.

53. Maller, J. J. *et al.* Occipital bending in schizophrenia. *Australian and New Zealand Journal of Psychiatry* **51**, 32–41 (2017).

54. van Haren, N. E. M. *et al.* Progressive Brain Volume Loss in Schizophrenia Over the Course of the Illness: Evidence of Maturational Abnormalities in Early Adulthood. *Biological Psychiatry* **63**, 106–113 (2008).

55. Gutiérrez-Galve, L. *et al.* A longitudinal study of cortical changes and their cognitive correlates in patients followed up after first-episode psychosis. *Psychological Medicine* **45**, 205–216 (2015).

56. Schobel, S. A. *et al.* Imaging Patients with Psychosis and a Mouse Model Establishes a Spreading Pattern of Hippocampal Dysfunction and Implicates Glutamate as a Driver. *Neuron* **78**, 81–93 (2013).

57. Sadeghi, D. *et al.* An overview of artificial intelligence techniques for diagnosis of Schizophrenia based on magnetic resonance imaging modalities: Methods, challenges, and future works. *Computers in Biology and Medicine* vol. 146 Preprint at https://doi.org/10.1016/j.compbiomed.2022.105554 (2022).

58. McGuire, P., Howes, O. D., Stone, J. & Fusar-Poli, P. Functional neuroimaging in schizophrenia: diagnosis and drug discovery. *Trends in Pharmacological Sciences* vol. 29 91–98 Preprint at https://doi.org/10.1016/j.tips.2007.11.005 (2008).

59. Frodl, T. *et al.* Reduced gray matter brain volumes are associated with variants of the serotonin transporter gene in major depression. *Molecular Psychiatry* **13**, 1093–1101 (2008).

60. Goldstone, A. *et al.* The mediating role of cortical thickness and gray matter volume on sleep slow-wave activity during adolescence. *Brain Structure and Function* **223**, 669–685 (2018).

61. Pontillo, G. *et al.* Unraveling deep gray matter atrophy and iron and myelin changes in multiple sclerosis. *American Journal of Neuroradiology* **42**, 1223–1230 (2021).

62. Oh, H., Habeck, C., Madison, C. & Jagust, W. Covarying alterations in Aβ deposition, glucose metabolism, and gray matter volume in cognitively normal elderly. *Human Brain Mapping* **35**, 297–308 (2014).

63. Zhang, Y. *et al.* Cortical grey matter volume reduction in people with schizophrenia is associated with neuro-inflammation. *Translational Psychiatry* **6**, (2016).

64. Lotter, L. D. *et al.* Human cortex development is shaped by molecular and cellular brain systems. *bioRxiv* **17**, (2023).

65. Hansen, J. Y. *et al.* Mapping neurotransmitter systems to the structural and functional organization of the human neocortex. *Nature Neuroscience* **25**, 1569–1581 (2022).

66. Yang, H. *et al.* Connectional Hierarchy in Human Brain Revealed by Individual Variability of Functional Network Edges. *bioRxiv* (2023) doi:10.1101/2023.03.08.531800.

67. Luppi, A. I. *et al.* In vivo mapping of pharmacologically induced functional reorganization onto the human brain's neurotransmitter landscape. *Science Advances* (2023).

68. Onwordi, E. C. *et al.* Synaptic density marker SV2A is reduced in schizophrenia patients and unaffected by antipsychotics in rats. *Nature Communications* **11**, (2020).

69. Wischhof, L. & Koch, M. 5-HT2A and mGlu2/3 receptor interactions: On their relevance to cognitive function and psychosis. *Behavioural Pharmacology* vol. 27 1–11 Preprint at https://doi.org/10.1097/FBP.0000000000000183 (2016).

70. Luca, V. De, Viggiano, E., Dhoot, R., Kennedy, J. L. & Wong, A. H. C. Methylation and QTDT analysis of the 5-HT2A receptor 102C allele: Analysis of suicidality in major psychosis. *Journal of Psychiatric Research* **43**, 532–537 (2009).

71. Price, D. L., Bonhaus, D. W. & McFarland, K. Pimavanserin, a 5-HT2A receptor inverse agonist, reverses psychosis-like behaviors in a rodent model of Alzheimer's disease. *Behavioural Pharmacology* **23**, 426–433 (2012).

72. McFarland, K., Price, D. L. & Bonhaus, D. W. Pimavanserin, a 5-HT2A inverse agonist, reverses psychosis-like behaviors in a rodent model of Parkinson's disease. *Behavioural Pharmacology* **22**, 681–692 (2011).

73. Stevens, K. E., Wear, K. D., Stevens, K. E. & And, K. D. *Normalizing Effects of Nicotine and a Novel Nicotinic Agonist on Hippocampal Auditory Gating in Two Animal Models*. *Pharmacology Biochemistry and Behavior* vol. 57 (1997).

74. Geyer, M. A., Krebs-Thomson, K., Braff, D. L. & Swerdlow, N. R. Pharmacological studies of prepulse inhibition models of sensorimotor gating deficits in schizophrenia: A decade

in review. *Psychopharmacology* vol. 156 117–154 Preprint at https://doi.org/10.1007/s002130100811 (2001).

75. Radek, R. J., Kohlhaas, K. L., Rueter, L. E. & Mohler, E. G. *Treating the Cognitive Deficits of Schizophrenia with Alpha4Beta2 Neuronal Nicotinic Receptor Agonists*. *Current Pharmaceutical Design* vol. 16 (2010).

76. Mackowick, K. M. *et al.* Neurocognitive endophenotypes in schizophrenia: Modulation by nicotinic receptor systems. *Progress in Neuro-Psychopharmacology and Biological Psychiatry* vol. 52 79–85 Preprint at https://doi.org/10.1016/j.pnpbp.2013.07.010 (2014).

77. Wang, H. Y. *et al.* mGluR5 hypofunction is integral to glutamatergic dysregulation in schizophrenia. *Molecular Psychiatry* **25**, 750–760 (2020).

78. Nicoletti, F. *et al.* Targeting mGlu receptors for optimization of antipsychotic activity and disease-modifying effect in schizophrenia. *Frontiers in Psychiatry* **10**, (2019).

79. Whitaker, K. J. *et al.* Adolescence is associated with genomically patterned consolidation of the hubs of the human brain connectome. *Proceedings of the National Academy of Sciences of the United States of America* **113**, 9105–9110 (2016).

80. Stauffer, E.-M., Bethlehem, R. A., Dorfschmidt, L., Won, H. & Bullmore, E. T. The genetic relationships between brain structure and schizophrenia. *medRxiv* (2023) doi:10.1101/2023.03.13.23287137.

81. Selvaggi, P. *et al.* Reduced cortical cerebral blood flow in antipsychotic-free first-episode psychosis and relationship to treatment response. *Psychological Medicine* 1–11 (2022) doi:10.1017/s0033291722002288.

82. Kapellou, O. *et al.* Abnormal Cortical Development after Premature Birth Shown by Altered Allometric Scaling of Brain Growth. *PLOS Medicine* (2006) doi:10.1371/journal.pmed.

83. Sikela, J. M. & Searles Quick, V. B. Genomic trade-offs: are autism and schizophrenia the steep price of the human brain? *Human Genetics* **137**, 1–13 (2018).

84. Smiley, J. F., Konnova, K. & Bleiwas, C. Cortical thickness, neuron density and size in the inferior parietal lobe in schizophrenia. *Schizophrenia Research* **136**, 43–50 (2012).

85. Smiley, J. F. *et al.* Hemispheric comparisons of neuron density in the planum temporale of schizophrenia and nonpsychiatric brains. *Psychiatry Research - Neuroimaging* **192**, 1–11 (2011).

86. Germann, M., Brederoo, S. G. & Sommer, I. E. C. Abnormal synaptic pruning during adolescence underlying the development of psychotic disorders. *Current Opinion in Psychiatry* vol. 34 222–227 Preprint at https://doi.org/10.1097/YCO.0000000000000696 (2021).

87. Borgan, F. *et al.* In Vivo Availability of Cannabinoid 1 Receptor Levels in Patients with First-Episode Psychosis. *JAMA Psychiatry* **76**, 1074–1084 (2019).

88. Schobel, S. A. *et al.* Differential Targeting of the CA1 Subfield of the Hippocampal Formation by Schizophrenia and Related Psychotic Disorders. *Arch Gen Psychiatry* (2009).

89. Parellada, E. & Gassó, P. Glutamate and microglia activation as a driver of dendritic apoptosis: a core pathophysiological mechanism to understand schizophrenia. *Translational Psychiatry* vol. 11 Preprint at https://doi.org/10.1038/s41398-021-01385-9 (2021).

90. De Gregorio, D., Comai, S., Posa, L. & Gobbi, G. D-Lysergic Acid Diethylamide (LSD) as a model of psychosis: Mechanism of action and pharmacology. *International Journal of Molecular Sciences* vol. 17 Preprint at https://doi.org/10.3390/ijms17111953 (2016).

91. Madre, M. *et al.* Neuropsychological and neuroimaging underpinnings of schizoaffective disorder: a systematic review. *Acta Psychiatrica Scandinavica* vol. 134 16–30 Preprint at https://doi.org/10.1111/acps.12564 (2016).

92. Garavan, H. *et al.* Recruiting the ABCD sample: Design considerations and procedures. *Developmental Cognitive Neuroscience* **32**, 16–22 (2018).

93. Casey, B. J. *et al.* The Adolescent Brain Cognitive Development (ABCD) study: Imaging acquisition across 21 sites. *Developmental Cognitive Neuroscience* vol. 32 43–54 Preprint at https://doi.org/10.1016/j.dcn.2018.03.001 (2018).

94. Loughland, C. *et al.* Australian Schizophrenia Research Bank: a database of comprehensive clinical, endophenotypic and genetic data for aetiological studies of schizophrenia. *Australian and New Zealand Journal of Psychiatry* (2010) doi:10.3109/00048674.2010.501758.

95. Kristian Hill, S. *et al.* Neuropsychological impairments in schizophrenia and psychotic Bipolar disorder: Findings from the Bipolar-Schizophrenia Network on Intermediate Phenotypes (B-SNIP) study. *American Journal of Psychiatry* **170**, 1275–1284 (2013).

96. Poldrack, R. A. *et al.* A phenome-wide examination of neural and cognitive function. *Scientific Data* **3**, (2016).

97. Gollub, R. L. *et al.* The MCIC collection: A shared repository of multi-modal, multi-site brain image data from a clinical investigation of schizophrenia. *Neuroinformatics* **11**, 367–388 (2013).

98. Neilson, E. *et al.* Impact of Polygenic Risk for Schizophrenia on Cortical Structure in UK Biobank. *Biological Psychiatry* **86**, 536–544 (2019).

99. Fraser, A. *et al.* Cohort profile: The avon longitudinal study of parents and children: ALSPAC mothers cohort. *International Journal of Epidemiology* **42**, 97–110 (2013).

100. Sharp, T. H. *et al.* Population neuroimaging: Generation of a comprehensive data resource within the ALSPAC pregnancy and birth cohort. *Wellcome Open Research* **5**, (2020).

101. Horwood, J. *et al.* IQ and non-clinical psychotic symptoms in 12-year-olds: Results from the ALSPAC birth cohort. *British Journal of Psychiatry* **193**, 185–191 (2008).

102. Zammit, S. *et al.* Investigating if psychosis-like symptoms (PLIKS) are associated with family history of schizophrenia or paternal age in the ALSPAC birth cohort. *Schizophrenia Research* **104**, 279–286 (2008).

103. Wing, J. K., Babor, T., Brugha, T., Burke, J. & Sartorius, N. SCAN. Schedules for Clinical Assessment in Neuropsychiatry. *Archives of General Psychiatry* **47**, 589 (1990).

104. Crespo-Facorro, B. *et al. A Practical Clinical Trial Comparing Haloperidol, Risperidone, and Olanzapine for the Acute Treatment of First-Episode Nonaffective Psychosis. J Clin Psychiatry* vol. 67 (2006).

105. Rodriguez-Perez, N. *et al.* Long term cortical thickness changes after a first episode of non- affective psychosis: The 10 year follow-up of the PAFIP cohort. *Progress in Neuro-Psychopharmacology and Biological Psychiatry* **108**, (2021).

106. First, M., Spitzer, R., Gibbon, M. & Williams, J. Structured Clinical Interview for DSM-IV Axis I Disorders (SCID-I). (1996).

107. Canal-Rivero, M. *et al.* Longitudinal trajectories in negative symptoms and changes in brain cortical thickness: 10-year follow-up study. *The British Journal of Psychiatry* 1–10 (2023) doi:10.1192/bjp.2022.192.

108. Ayesa-Arriola, R. *et al.* Erratum: Dissecting the functional outcomes of first episode schizophrenia spectrum disorders: a 10-year follow-up study in the PAFIP cohort - CORRIGENDUM (Psychological medicine (2021) 51 2 (264-277)). *Psychological medicine* vol. 51 278 Preprint at https://doi.org/10.1017/S0033291719003854 (2021).

109. Benjamini, Y. & Hochberg, Y. *Controlling the False Discovery Rate: A Practical and Powerful Approach to Multiple Testing. Source: Journal of the Royal Statistical Society. Series B (Methodological)* vol. 57 (1995).

110. Markello, R. D. *et al.* neuromaps: structural and functional interpretation of brain maps. *Nature Methods* **19**, 1472–1479 (2022).

111. Shafiei, G. *et al.* Neurophysiological signatures of cortical micro-architecture. *Nature Communications* **14**, 6000 (2023).

112. Krishnan, A., Williams, L. J., McIntosh, A. R. & Abdi, H. Partial Least Squares (PLS) methods for neuroimaging: A tutorial and review. *NeuroImage* **56**, 455–475 (2011).

113. McIntosh, A. R. & Lobaugh, N. J. Partial least squares analysis of neuroimaging data: Applications and advances. in *NeuroImage* vol. 23 (2004).

Author Contributions

N.G.S. performed data curation, methodological design, data analysis, and drafted the manuscript; R.A.I.B., A.M., J.S., I.S., C.A.M., L.D., G.S., V.O.G., K.M., A.D., S.E.M., M.R.V., R.A.A., J.V.B., A.A.B., B.M., E.T.B., J.S., B.C.F., and R.R.G contributed to data acquisition, provided advice on data analysis, and participated in writing and editing the manuscript. R.R.G. also contributed to conceptualization and supervision of the work. All authors approved the submitted version of the manuscript.

Acknowledgments

RRG is funded by the EMERGIA Junta de Andalucía program (EMERGIA20_00139), the Plan Propio of the University of Seville and the Plan de Generación de Conocimiento from the Spanish Ministry of Science (PID2021-122853OA-I00).

Competing Interests

The authors declare no competing interests in relation to the work described.